RESEARCH ARTICLE

Antibacterial and Healing Efficacy of Mangiferin-Loaded Silver Nanoparticle and Chitosan-Alginate Membrane Dressings

Manisha Khaire, Papiya Bigoniya*

DSKM College of Pharmacy, Faculty of Pharmacy, RKDF University, Bhopal, Madhya Pradesh, India.

Received: 13th March, 2024; Revised: 24th May, 2024; Accepted: 17th June, 2024; Available Online: 31st August, 2024

ABSTRACT

Mangiferin, a bioactive constituent of *Mangifera indica* (family Anacardiaceae), has an impressive therapeutic profile, having antioxidant, anti-inflammatory, analgesic, antibacterial, and immunomodulatory properties capable of possessing wound healing potential. Our investigation aims to isolate and characterize mangiferin, green synthesis of silver nanoparticles (Ag-NPs) and production of chitosan alginate (Cs/Alg) film dressing loaded with mangiferin Ag-NPs and assess antibacterial and wound-healing properties against infected excision and burn wounds. The isolated mangiferin was authenticated by estimating melting point, thin layer chromatography (TLC), fourier-transform infrared spectroscopy (FTIR), and high-performance liquid chromatography (HPLC). Ag-NPs were green synthesized and characterized by UV-visible, particle size, zeta potential (ZP), entrapment efficiency (%EE), scanning electron microscope (SEM), transmission electron microscope (TEM), and stability study. Chitosan alginate membrane dressing was prepared by incorporating mangiferin Ag-NPs, and film thickness, pH, film weight, water intake capacity, and *in-vitro* drug release parameters were estimated. Among the four mangiferin Ag-NP batches, MN3 formed stable polydispersity spherical Ag-NPs with smaller particle size and high %EE. Mangiferin-loaded Cs/Alg film MN-CM4 showed significantly higher ($p < 0.001$) drug content, wettability, release profile, and favorable pH changes. The mangiferin Ag-NPs embedded Cs/Alg film dressing showed a significantly high antimicrobial effect against the gram-positive bacterial strain of *S. aureus,* commonly found in wounds. MN3 and MN-CM4 treatment showed the shortest epithelialization period and enhanced wound closure. The hydroxyproline content has significantly ($p < 0.001$) increased, and myeloperoxidase content was reduced by MN3 and MN-CM4 treatment. MN-CM4 treatment showed complete re-epithelialization reduced inflammatory cells with thicker and denser collagen fiber deposition. The effectiveness of the Cs/Alg film of mangiferin Ag-NPs dressing has a synergistic effect on promoting speedy wound healing. The Cs/Alg film of mangiferin Ag-NPs showed rapid wound healing against infected and burned wounds, enhanced collagen synthesis, and anti-inflammatory and antibacterial efficacy.

Keywords: Mangiferin, Silver nanoparticles (Ag-NPs), Chitosan alginate (Cs/Alg) film, Infected excision wound, Burn wound, Wound healing.

International Journal of Pharmaceutical Quality Assurance (2024); DOI: 10.25258/ijpqa.15.3.127

How to cite this article: Khaire M, Bigoniya P. Antibacterial and Healing Efficacy of Mangiferin-Loaded Silver Nanoparticle and Chitosan-Alginate Membrane Dressings. International Journal of Pharmaceutical Quality Assurance. 2024;15(3): 1948-1961.

Source of support: Nil.

Conflict of interest: None

INTRODUCTION

Nano-science and nanotechnology are rapidly developing fields of medical science with unique characteristics and capabilities due to atom arrangements on a size of 1 to 100 nm. Nanotechnology, particularly in wound healing, offers non-adherence to the wound surface, flexibility, high porosity, and appropriate mechanical strength.[1] Ag-NPs are inorganic noble metal particles with promising uses in arenas, for example, chemistry, physics, environmental cleanup, optoelectronics, materials science, biomedical devices, and renewable energy. Their unique physicochemical properties, for example, size, structure, and antibacterial and antioxidant capability, make AgNPs particularly interesting.[2] Nanoparticles influence the healing mechanism by affecting collagen deposition and realignment and start the process of skin regeneration. Their moisturizing qualities, cooling sensations, and resistance against microbial contamination are other appealing attributes.[3]

Chitosan is obtained from chitin, a naturally arising biopolymer that is a significant part of the exterior exoskeleton of crustaceans. Chitosan is widely recognized for its hemostatic properties in wound treatment. Additionally, it exhibits various biological activities and affects macrophage function, leading to faster wound healing. Chitosan also supports tissue organization and cell proliferation within histoarchitecture. Biological qualities, for example fungi-static and bacteriostatic when treating wounds are beneficial. Like alginate material,

*Author for Correspondence: p_bigoniya2@hotmail.com

chitosan has been the subject of several references for wound therapy. When new chitosan–alginate polyelectrolyte complex (PEC) membranes were employed instead of traditional gauze dressings, rat model excision wounds healed more quickly.[5]

Alginate may be prepared into various shapes, including fibers, films, and microspheres. -OH- groups alongside the alginate mainstay facilitate crosslinking with compounds like glutaraldehyde and 1,6-hexane diamine. However, alginates have limitations, for example higher water solubility in addition to low mechanical strength. Previously, reinforced chitosan was created by combining alginates' anionic -COOH- groups with chitosan's cationic -NH- groups. The resulting chitosan/alginate polyelectrolyte complex is used in wound care and drug delivery. This work produced chitosan/alginate membranes with varying molar ratios utilizing both covalent and ionic crosslinking. Several characterization tools were used to characterize the membranes.[6] Chitosan and alginate-based wound dressings are well recognized in scientific and commercial domains for their effectiveness in wound care. Alginate's ability to form gels makes removing the dressing less painful for the patient and allows for removing the dressing with less damage. It offers a damp atmosphere that promotes quick granulation and reepithelialization.[5]

Mangiferin is a C-glucosylxanthone biosynthesized in the leaf, bark, flower, and root of the mango tree, especially in fruit peel, pulp, and seed. Chemically, 2-C-β-D-gluco-pyranosyl-1, 3,6,7-tetrahydroxy xanthone, mangiferin is present in many plant species but abundantly isolated from *Mangifera indica* (family Anacardiaceae). The C-glucosyl xanthone, which resembles the unique structural characteristics of biflavones, has excellent nutritional and medicinal value. The c-glycoside bond of mangiferin is analogous to nucleophilic phloroglucinol substitution, enhancing its bioavailability and conferring antioxidant characteristics.[7] Mangiferin has impressive therapeutic properties as an antioxidant, anti-inflammatory, analgesic, antibacterial, antiviral, immunomodulatory, anticancer, antidiabetic, and hepatoprotective.[8-17] Would the healing, anti-inflammatory, and antibacterial effect of mangiferin contrary to gram-positive and gram-negative microorganisms and its ability to improve epidermis and dermis architecture make it suitable for wound dressing. By preventing infection at the wound site, mangiferin may facilitate optimal conditions for remedial in addition to decreasing the threat of impediments.[19] Analgesic and anti-inflammatory qualities of mangiferin are well documented.[20] Mangiferin gel facilitated diabetic wound healing by increasing the expression of EGF, FGF, TGF-β, VEGF, PI3K, MMP, and Nrf2. On the other hand, decreasing TNFα and NF-κB p65 expression.[21] Mangiferin-incorporated glycoltransfersomes enhanced mangiferin deposition in the epidermis and dermis, shielded fibroblasts from oxidative stress, and promoted their proliferation on skin lesions.[22] Mangiferin exhibits moderate aqueous solubility and low lipophilicity.[23]

Mangiferin can be formulated into various delivery systems, including films, gels, and creams, to enhance its bioavailability and efficacy at the wound site. Film formulations offer the advantage of providing sustained release of mangiferin, ensuring prolonged exposure to its beneficial effects. Overall, the combination of anti-inflammatory, antioxidant, antimicrobial, collagen-stimulating, and moisture-retaining properties makes mangiferin a promising candidate for wound healing films. Mangiferin-containing films could help retain moisture at the wound site, which is essential for cell migration, proliferation, and tissue redevelopment. Ag-NPs derived from *M. indica* flower extract have potential antibacterial activity.[24] Mangiferin Ag-NPs demonstrated antioxidant and antibacterial action in contradiction of *S. aureus* and *E. coli*.[25,26]

Chalitangkoon *et al*. (2020) created hydrogel films composed of Ag-loaded hydroxyethylacryl chitosan and SA to facilitate controlled drug release in wound dressings.[27] Additionally, Pansara *et al*. (2020) developed wound-healing films incorporating Ag-NP embedded in chitosan and inspected *in-vivo* and *in-vitro* characteristics[28]. However, the green-synthesized mangiferin Ag-NP embedded in chitosan, potentially offering synergistic antibacterial effects, is currently unavailable. Our investigation aims to isolate and characterize the prospective plant with bioactive phytoconstituents known for wound healing and antibacterial properties. Additionally, Ag-NP will be synthesized utilizing green methods with the assistance of these isolated phytoconstituents, and their formulation and characterization will be conducted. Furthermore, a chitosan alginate dressing loaded with Ag-NP derived from the isolated phytoconstituents is being developed and evaluated for its effectiveness in wound healing.

MATERIALS AND METHODS

Material

The Mango leaves were received from Wadachi Wadi, Pune, Maharashtra, India, in September 2022 and authenticated by Dr. Lad Meenal Deepak, College of Ayurveda and Research Centre, Akurdi, Pune. A specimen was filed with reference no.1482/2023-2024 for future reference.

Methods

Extraction and isolation of mangiferin

Fresh Mango leaves were collected, shade-dried, and ground into a coarse powder. The dried crude material was extracted utilizing petroleum ether (60–80°C) as a solvent utilizing the Soxhlet extraction technique for 24 hours. The defatted marc was extracted under reflux for 20 hours utilizing ethanol (70%). After overnight settling, the solid was filtered and washed with petroleum ether to yield a yellow crude extract. Recrystallization in ethyl acetate (EA) and methanol produced pale yellow crystals, and the yield was calculated.[29]

Characterization of isolated mangiferin

- *Organoleptic properties*

Organoleptic properties, for example color, odor, and physical nature of the isolated compound, were visually observed. A

small amount of mangiferin was placed on butter paper and viewed in a well-illuminated area.

- *Melting point*

The melting point of mangiferin was estimated utilizing the Capillary technique with a Thieles tube melting apparatus (Oswal Scientific, Pune). Readings are taken in triplicate.[30]

- *Thin layer chromatography (TLC)*

Chromatographic separation used a Camag TLC chamber with a 10 × 10 cm silica gel plate (100 µm). Samples were applied utilizing a Camag Linomat applicator, and various mixtures of ethyl acetate, acetic acid, formic acid, and water served as mobile phases. TLC plates were dried at 25°C, and mangiferin was scanned densitometrically at 262 nm.[31]

- *Calibration curve*

Isolated mangeferin dilutions were prepared in the 100 to 500 µg/mL range. Absorbance was noted on the JASCO V-530, UV-vis spectrophotometer, Japan, in the 200 to 400 nm wavelength range. Absorbance values were plotted versus concentration and analyzed for regression coefficient.[32]

- *Fourier-transform infrared spectroscopy*

The fourier-transform infrared spectroscopy (FTIR) spectra were documented in the range of 4000 to 400 cm^{-1} utilizing a JASCO - 460 plus FTIR spectrophotometer (Japan) with diffuse reflectance. The FTIR spectra of the isolated mangiferin were then compared with the reported spectrum.[33]

- *High-performance liquid chromatography*

The chromatographic system used an LC-10AT HPLC (Shimadzu) with an SPD-20A UV detector and an Inertsil ODS-SP column (250 × 4.6 mm, 5 µm). The mobile phase was methanol and 0.1% phosphoric acid (31:69, v/v). Mangiferin stock solution was prepared in methanol, and working standards were diluted to 0.76, 3.82, 19.10, 95.52, and 477.60 mg/mL, stored at 4°C. After 30 minutes of ultrasonic extraction, the sample was cooled and filtered through a 0.45 µm membrane. Analyses were conducted at 258 nm with a flow rate of 1.0 mL/min at room temperature (RT).[34]

- *Green synthesis of mangiferin -Ag-NPs*

A measured amount of mangiferin was combined with 2M NaOH to create a mangiferin oxide solution, which was then added drop by drop into a 0.5% silver nitrate solution with continuous stirring for several hours. The color change from yellow to brown indicated the formation of Ag-NP. Afterward several hours of stirring, the reduction was complete. The solution was centrifuged at 4000 rpm for 30 minutes, the supernatant was decanted, and the residue was washed away thrice in the direction of eradicating impurities. The precipitate was washed with deionized water, filtered through a membrane, and dried under a vacuum to obtain pure Ag-NPs. Four batches of mangiferin Ag-NPs were formulated with mangiferin concentrations of 0.05, 0.075, 0.1, and 0.15 g/mL, designated as MN1, MN2, MN3, and MN4, respectively.[35,36]

Characterization of mangiferin -Ag-NPs

- *Particle size and zeta potential (ZP)*

The size of the particle and ZP (surface charge) of the mangiferin Ag-NPs were measured utilizing a Zetasizer Nano ZS (Malvern Instruments, UK). The nanoparticle formulations were diluted with 0.1 mL of water to determine the zeta potential and placed in an electrophoretic cell with an electric field strength of 15.5 V/cm.

- *Entrapment efficiency (%EE)*

The EE of mangiferin in Ag-NPs was assessed utilizing ultracentrifugation. Mangiferin Ag-NPs were separated from the seeding solution by ultracentrifugation at 10,000 rpm for 30 minutes. The resultant pellets were re-dissolved in distilled water, and the mangiferin concentration in the supernatant was measured utilizing UV spectrophotometry. The %EE of mangiferin was then estimated utilizing this equation.[37]

% EE = Experimental mangiferin content / Theoretical mangiferin content × 100 ---------- (1).

- *Scanning electron microscopy (SEM)*

Mangiferin Ag-NPs were spread on 10 mm glass slides in addition to allowable to dry at ambient temperature in a vacuum desiccator for the whole night before being subjected to SEM analysis. The nanoparticles were placed on the proper support and coated with gold to a thickness 100 A°. Coated samples were analyzed utilizing an SEM (JEOL JSM-6360A, Singapore) operated at 15 KV, and photographs were captured.

- *TEM*

The morphology of the mangiferin Ag-NPs was analyzed using a TEM (JEOL-JEM 2100). Samples were prepared by air-drying diluted Ag-NP solution on carbon sheets on copper grids. TEM images were captured at 120 kV.

- *Stability of Ag-NPs*

The stability of the optimized batch of mangiferin Ag-NPs was assessed after 3 months of storage in a stability chamber at 30 ± 2°C and 65 ± 5% RH. Measurements of particle size, ZP, %EE, and physical appearance were taken at 1, 2, and 3-month intervals.[38]

- *Mangiferin Chitosan/Alginate (Cs/Alg) membrane*

Chitosan/alginate polyelectrolyte membranes were prepared utilizing the solution casting-solvent evaporation method for covalent crosslinking and physical mixing. Activated low molecular weight alginate was prepared following the method reported.[38] A 3% chitosan solution (in 2% glacial acetic acid) was combined with activated alginate in molar ratios of 4:1, 3:1, 2:1, and 1:1. The mixture was stirred at 1,000 rpm for 30 minutes at ambient temperature, and the pH adjusted to 5.5 with HCl. Viscosity was measured at 100 rpm using a Brookfield Viscometer at 25°C. To each of these four solutions, 0.2 mL of MF-Ag-NP solution was added while stirring to ensure complete homogeneity. The solutions were deaerated, poured

onto a glass plate, and dried at RT. The crosslinked Cs/Alg membranes were then washed with methanol and vacuum-dried at 40°C for 5 hours. The mangiferin Ag-NP-loaded membranes were labeled MN-CM1, MN-CM2, MN-CM3, and MN-CM4.[38]

Characterization of mangiferin Cs/Alg membrane

- *Membrane thickness*

An Elcometer 456 coating thickness gauge measured film thickness in both dry and wet states. Measurements were taken at various locations on the sample, both before and after wetting, at intervals of 15 min., 1, 3, 8, and 24 hours.[39]

- *Membrane weight and uniformity of mass*

Twenty 2.5 × 2.5 cm pieces were cut from arbitrary parts of the films. The average mass ± SD was measured utilizing an analytical scale (GR-202, A&D Company Ltd., India), and %deviation from the average mass was calculated.[39]

- *Water uptake capability*

Each film was weighed three times, equilibrated in 15 mL of PBS (pH 7.4) at RT for 24 hours, and then re-weighed after blotting excess water. This was repeated until constant weight was achieved. The percentage of water uptake was then calculated:

Percent water uptake = [(WW-DW)/DW] × 100 ------ (2).
Where, DW: Dry Weight; WW: Wet Weight

- *Drug content*

Drug content uniformity was tested by dissolving a 10 mm film in 100 mL isotonic PBS pH 7.4 and homogenizing for 6 hours with occasional shaking. A 5 mL aliquot was diluted to 20 mL with PBS pH 6.8, filtered through a 0.45 µm filter, and analyzed at 257 nm using UV spectrophotometry.[43]

%mangiferin content = Experimental mangiferin content/ Theoretical mangiferin content × 100 ------ (3).

- *Membrane surface pH*

The surface pH of the films was measured with a contact pH meter (Flatrode, Hamilton) after wetting with a drop of purified water at various intervals over 24 hours.[44]

- *In-vitro drug release*

In-vitro drug release was studied using a Franz Diffusion cell with mangiferin Cs/Alg membranes (1 × 1 cm) placed on a cellulose acetate membrane. The receptor compartment contained PBS pH 7.4 at room temperature. Samples were collected over 24 hours and analyzed by UV spectrophotometry at 257 nm. Fresh PBS was added after each sample to maintain sink conditions.[45]

- *Antibacterial activity*

The agar diffusion technique assessed the antibacterial activity of the mangiferin Cs/Alg membrane. Suspensions of *A. niger, E. coli, P. aeruginosa*, and *S. aureus* in a final concentration of 108 cfu/mL (McFarland scale) were streaked evenly on the surface of Petri dishes containing Mueller-Hinton agar spending a cotton swab. After air drying for 5 minutes, the membrane (6 mm diameter disks) was placed on top of the swabbed media and incubated overnight at 37°C. Afterwards incubation, the antibacterial activities of the membrane were determined by measuring the inhibition zones formed. The experiments were triplicate.[46,47]

Wound healing activity

- *Experimental animals*

Wister Albino rats of either sex weighing between 200 to 240 gm (12–16 weeks) were used for animal study. The rats were acclimatized to the animal house condition for one week before doing any experimental work. The rats were fed water and a regular animal pellet diet (VRK Nutritional Solution, Pune). They were housed at RT (24 ± 2°C), RH (50 ± 5%), and 12 hours light and dark cycle. Study protocols were prepared by the ethical guidelines of the CPCSEA (CPCSEA Registration No: 1988/PO/Re/S/17/CPCSEA) and approved by IAEC (Approval No: GIPER/IAEC/22/06). [48]

- *Infected excision wound*

On the day of wound creation, 36 rats were randomly assigned to six groups: Group 1 (wound control), group 2 (infected wound control), group 3 (Ag-NPs), group 4 (MN-3), group 5 (Cs/Alg membranes), and group 6 (MN-CM4). The rats were anesthetized with ketamine (80 mg/kg, IP) and diazepam (5 mg/kg, IP), and wounds were created on their dorsal thoracic region, 1 cm from the vertebral column, utilizing a scalpel and scissors. After hemostasis was achieved, the wounds were left exposed. On day 14, the excised skin was collected for histological and biochemical analysis. Wounds were inoculated with Staphylococcus aureus (1×10^6 CFU/mL) except for the wound control group. Treatments began on day 3, with the control groups receiving 0.9% saline. Groups 3 and 4 were treated daily with Ag-NP, while groups 5 and 6 were treated with pre-moistened chitosan-alginate films, which were covered with gauze and tape. The films were replaced on days 4, 7, 14, and 21 after hydration with saline and light anesthesia.[48]

- *Burn wound*

Thirty experimental animals were divided into five groups: Group 1 (burn wound control), group 2 (Ag-NPs), group 3 (MN-3), group 4 (Cs/Alg membranes), and group 5 (MN-CM4). A deep burn wound (15 mm diameter, 177 mm^2) was created on the dorsal surface utilizing an electrical heater at 110°C for 10 seconds, and the skin was cleaned with normal saline. Treatments began 24 hours after wounding, which was designated as day 1. The burn wound control group was treated with 0.9% saline (150 µL) and covered with gauze and tape. Groups 2 and 3 received daily applications of a silver nanoparticle formulation and were left uncovered. Groups 4 and 5 were treated with chitosan-alginate films (2 cm diameter)

pre-moistened with 0.9% saline (100 µL), and all wounds were enclosed with gauze and tape, which were altered day-to-day with saline hydration until the 7th follow-up day. Films were replaced on days 4, 7, 14, and 21 under light anesthesia. Burned skin was collected on day 14 for histological and biochemical analysis, and the wound healing properties were assessed by measuring wound area, contraction, epithelialization period, myeloperoxidase, hydroxyproline levels, and skin histology in both burn and infected excision wound models.[48]

- *Wound area*

The wound area was measured with translucent paper on a 1-mm² graph sheet on days 1, 4, 7, 14, and 21, then every other day until closure. Wound contraction was calculated as a percentage of the initial size. Phlogistic characteristics like infiltration, edema, abscess, lesions, and exudates were monitored every 48 hours.[48]

- *Wound contraction*

Wound closure was assessed by tracing the wound on specific days with transparent paper and a permanent marker. The traced areas were measured with 1-mm² graph paper to determine the wound contraction rate and epithelialization period, calculating the percentage of contraction relative to the initial wound size.[48]

%Wound closure = (WA on 1st day − WA on day (n) / WA on 1st day × 100 ---------- (4).
Where, n is the number of days (2nd, 4th, etc.) and WA: Wound Area

- *Epithelialization period*

The detachment of the scab, with no raw wound remaining, was considered the endpoint of complete epithelialization. The number of days mandatory for this to occur was recorded as the epithelialization period.[48]

- *Myeloperoxidase assay*

Skin samples were stored in Eppendorf flasks with an ice-cold buffer (0.1M NaCl, 20 mM NaPO4, 15 mM Na EDTA, pH 4.7) at 28°C. Absorbance was measured at 450 nm using a 96-well microplate reader. Results were reported as PMNs × 10³ cells/mg of tissue, equated to a standard curve.[50]

- *Hydroxyproline content*

Skin samples were incubated at 60°C for 15 hours, then homogenized with 6N hydrochloric acid and incubated at 130°C for 4 hours. After cooling and pH adjustment to 7.0, hydroxyproline standards (1.0–100 µg/mL) and samples were added to a 96-well microplate. Absorbance at 550 nm was measured after adding chloramine-T and Ehrlich's reagent and equated to a standard curve to determine hydroxyproline concentration.[50]

- *Histological processing*

Skin samples were fixed in 3.7% buffered formaldehyde (pH 7.4) for 24 hours, then sectioned into 5 µm slices and stained with Hematoxylin and Eosin (HE) for histological analysis of inflammatory infiltrate, blood vessels, and fibroblasts.[50]

RESULT

Characterization of Isolated Mangiferin

Isolated mangiferin (yield 1.3%) was obtained as pale-yellow needle-shaped crystals with melting points between 270 to 272ºC. TLC of mangiferin in EA, AA, FA, and water (7:1:1:1) showed RF value of 0.65 as standardized earlier by Khurana *et al*. (2016). Mangiferin showed maximum absorbance at 257 nm (Rasyid *et al*., 2020). The calibration curve of mangiferin showed linearity between absorbance and concentration with a regression coefficient of 0.9969. FTIR spectra of mangiferin showed IR U_{max} (KBr) cm^{-1}: 3331.81 (OH), 1621.89 (C=O), 1329.30 (CH-CH bending), 1216.63 (C-O). The IR spectra of mangiferin confirm the structure as per the reference standard reported by Othman and Sekar (2019). HPLC of mangiferin performed following the method reported by Zhang *et al*. (2014) showed Rt at 7.920 minutes equated to 8.166 minutes (Figures 1-4).

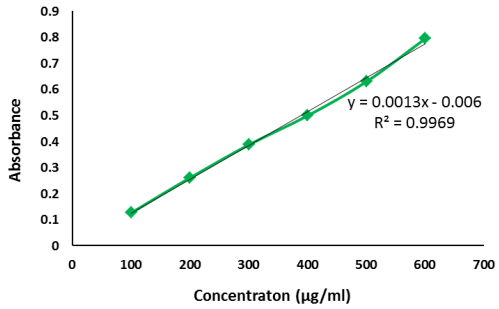

Figure 1: Calibration curve of mangiferin

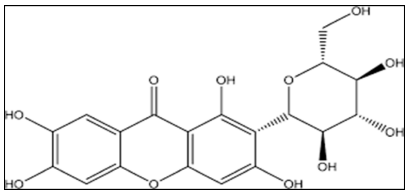

Figure 2: Chemical structure of mangiferin

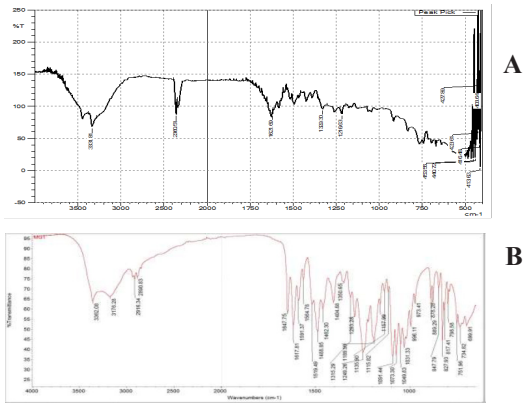

Figure 3: FTIR spectra of isolated mangiferin (A) and reference mangiferin (B) reported in Othman and Sekar (2019)

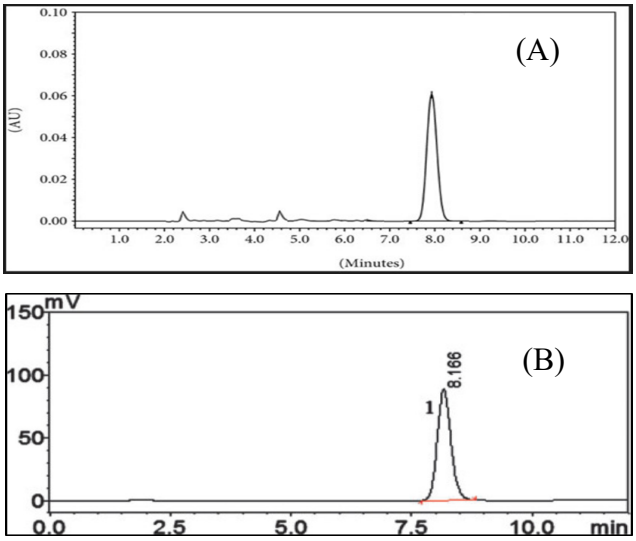

Figure 4: HPLC spectra of isolated mangiferin (A) and standard mangiferin (B) reported in Zhang *et al*. (2014)

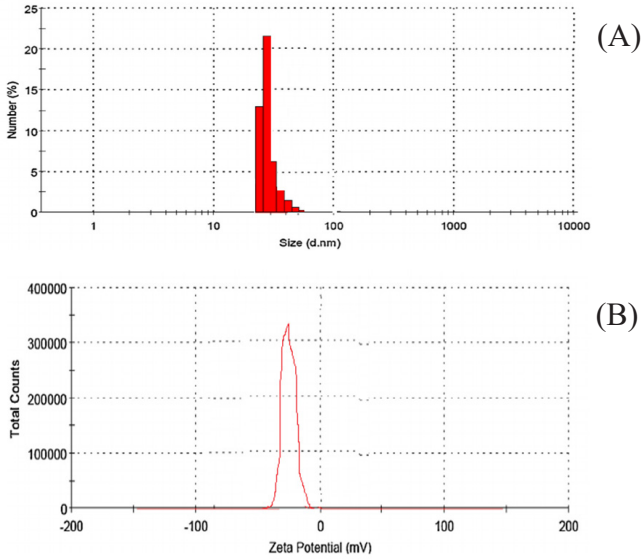

Figure 5: Particle density index (A) and zeta potential (B) of mangiferin-loaded nanoparticle batch MN3

Characterizations of Mangiferin Ag-NPs

The particle size of mangiferin Ag-NPs was found to be between 1 to 100 nm. Amongst the four batches of mangiferin Ag-NPs, MN3 shows (p <0.01) smaller average particle size, i.e., 36.60 ± 0.91 nm significantly, equated to other batches. Batch MN4 and MN3 displayed a noteworthy upsurge (p <0.001) in the zeta potential, respectively -39.24 and -29.10 mV signifying higher electrical stability. The MN3 batch showed significantly (p <0.01–0.001) high mangiferin entrapment efficiency of 77.42 and 74.18% product yield. SEM showed spherical-shaped smooth surface morphology of MN3 Ag-NPs. The TEM morphology of the synthesized Ag-NPs MN3 showed spherical uniform-sized nanoparticles having discrete nonaggregate appearance (Table 1, Figures 5 and 6).

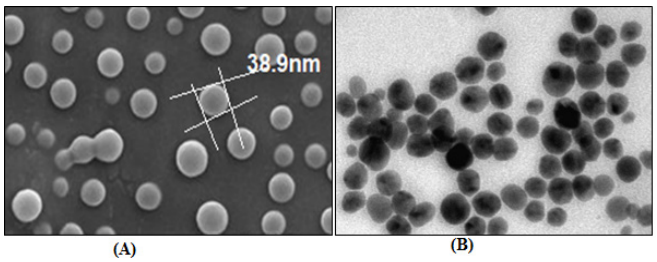

Figure 6: Scanning electron micrograph (A) and transmission electron microscopy (B) of mangiferin-loaded silver nanoparticle batch MN3

Stability of Mangiferin Ag-NPs MN3

There were no significant changes in mangiferin %EE, particle size and ZP of Ag-NPs batch MN3 over the storage period of three months (Table 2).

Characterization of Mangiferin Cs/Alg Membrane

The thicknesses of all films (MN-CM1 to MN-CM4) in the dry state ranged from 91.20 to 98.44 µm. The film thickness of all the formulations increased significantly (p <0.001) after wetting from 15 minutes to 24 hours duration. The average weight of prepared film samples varies from 70.42 to 95.21 mg. Formulation MN-CM4 showed significantly higher (p <0.001) weight and drug content (97.33%). The water uptake capability of all the formulations was in a similar range. The water absorption capacity of MN-CM4 was found to be higher, which consists of a 1:1 chitosan alginate ratio. The pH of all the batches showed significant change with time. The pH of MN-CM4 increased from 2.67 to 4.39 following 24 hours (Tables 3, 4 and 5).

In-vitro Drug Release

The MN-CM1 and MN-CM2 batches show moderately significant increases in drug release during the first hour, and from the second hour until six hours, the release profile was significantly higher. The MN-CM3 batch shows no significant

Table 1: Characterizations of mangiferin Ag-NP batches

Batch No	*Mangiferin (mg/mL)*	*Yield (%)*	*Particle size (nm)*	*Zeta potential (mV)*	*Entrapment efficiency (%)*
MN1	50	62.54 ± 0.54	40.02 ± 0.61	-23.17 ± 0.37	65.23 ± 0.87
MN2	75	71.84 ± 0.42*	52.67 ± 0.88***	-20.61 ± 0.7^{1**}	65.60 ± 0.67^{ns}
MN3	100	74.18 ± 1.0^{8**}	36.60 ± 0.91**	-29.10 ± 0.43***	77.42 ± 0.93***
MN4	150	70.32 ± 1.17*	46.39 ± 1.34***	-39.24 ± 1.0^{0***}	73.89 ± 1.06**

Values are expressed as Mean ± SD for 3 observations (n = 3). * p <0.05, ** p <0.01, *** p <0.001, and ns = not significant when equated to MN1 group values.

Table 2: Stability study of optimized mangiferin silver nanoparticle batch MN3

Storage time	*0 Day*	*1 Month*	*2 Month*	*3 Month*
Particle size (nm)	36.70 ± 0.11	36.80 ± 0.55^{ns}	36.60 ± 0.17^{ns}	36.60 ± 0.66^{ns}
ZP (mV)	−29.11 ± 0.05	−29.10 ± 0.18^{ns}	−29.11 ± 0.77^{ns}	−29.10 ± 0.79^{ns}
(%EE)	77.44 ± 0.73	77.42 ± 0.15^{ns}	77.43 ± 0.52^{ns}	77.42 ± 0.35^{ns}

Values are expressed as mean ± SD for 3 observations (n = 3). ns = not significant when equated to the respective zero day values.

Table 3: Film thickness of mangiferin chitosan alginate membrane batches

Batch No.	*Thickness (µm)*					
	Dry state	*15 minutes*	*1 hour*	*3 hours*	*8 hours*	*24 hours*
MN-CM1	91.82 ± 0.65	154.22 ± 0.78***	179.45 ± 0.34***	235.71 ± 0.28***	248.85 ± 0.45***	385.91 ± 0.37***
MN-CM2	91.20 ± 0.24	233.61 ± 0.26***	236.46 ± 0.76***	255.38 ± 0.15***	254.52 ± 0.37***	402.24 ± 0.13***
MN-CM3	96.51 ± 0.13	197.17 ± 0.18***	266.63 ± 0.34***	289.82 ± 0.62***	304.79 ± 0.16***	468.37 ± 0.48***
MN-CM4	98.44 ± 0.43	175.55 ± 0.45***	191.22 ± 0.16***	192.36 ± 0.56***	280.96 ± 0.29***	335.73 ± 0.67***

Values are expressed as mean ± SD for 3 observations (n = 3). *** $p < 0.001$ when equated to the dry state group values.

Table 4: Film weight, water uptake and drug content of mangiferin chitosan alginate membrane batches

Batch No.	*Weight (mg)*	*Water uptake (%)*	*Drug content (%)*
MN-CM1	70.42 ± 0.29	18.34 ± 0.26^{ns}	92.03 ± 0.16
MN-CM2	87.27 ± 0.37**	17.04 ± 0.84^{ns}	94.12 ± 0.38*
MN-CM3	94.60 ± 0.12**	18.09 ± 0.36^{ns}	94.50 ± 0.72*
MN-CM4	95.21 ± 0.58***	19.67 ± 0.12^{ns}	97.33 ± 0.21***

Values are expressed as mean ± SD for 3 observations (n = 3). * $p < 0.05$, ** $p < 0.01$, *** $p < 0.001$, and ns = not significant when equated to MN-CM1 group values.

change in the release profile during the initial hour, and later on, the release profile increased extremely significantly until six hours. The MN-CM4 batch shows an extremely significant increase in drug release profile throughout the six-hour study (Figure 7).

Antibacterial Activity

MN-CM1 and MN-CM2 presented a zone of inhibition in the range of 11.22 to 17.20 mm against *S. aureus* and P. *aeruginosa,* whereas MN-CM3 showed a 13.25 to 18.33 mm inhibition zone against *A. niger* and *S. aureus*. MN-CM4 was the most effective formulation with 9.23 to 17.52 mm diameter of inhibition zone against all the tested microorganisms (Table 6).

Infected Excision Wound

The infected wound group showed a dramatic increase in wound area (+69.57%), indicating severe infection and inflammation hindering the healing process. The MN-CM4 group exhibited the most substantial wound contraction, demonstrating its potent anti-inflammatory and wound-healing possessions. The MN3 and MN-CM4 groups showed a significant reduction in the wound area, highlighting their efficacy in accelerating wound healing. The MN-CM4 group achieved complete wound closure (100% contraction), while the infected group still had a substantial wound area (-18.67 %) on day 21 (Table 7). The epithelialization period, a critical measure of wound healing efficiency, was shortest for the MN-CM4 group at 20.16 ± 0.78 days, indicating rapid wound healing. The infected wound group had the longest epithelialization period at 32.50 ± 1.74 days, reflecting the delayed healing due to infection. The silver nanoparticle and MN3 groups also showed relatively short epithelialization periods, promoting wound healing (Figure 8). A substantial decrease ($p < 0.01$) in hydroxyproline content was perceived in infected wound control, whereas myeloperoxidase content was elevated. All the silver nanoparticle and chitosan/alginate film-treated groups exhibited extremely substantial ($p < 0.001$) reversal of the content of hydroxyproline and myeloperoxidase (Figure 9).

Table 5: Alteration of pH in mangiferin chitosan alginate membrane batches

Batch No.	*Ph*					
	After wetting	*15 minutes*	*1 hour*	*3 hours*	*8 hours*	*24 hours*
MN-CM1	2.47 ± 0.08	3.70 ± 0.10*	3.40 ± 0.14*	3.65 ± 0.76*	3.88 ± 0.78*	4.52 ± 0.27**
MN-CM2	2.61 ± 0.16	3.83 ± 0.62*	3.45 ± 0.23*	3.68 ± 0.62*	3.89 ± 0.67*	4.30 ± 0.16**
MN-CM3	2.55 ± 0.21	3.94 ± 0.29**	3.39 ± 0.11*	3.65 ± 0.19*	3.67 ± 0.31*	4.25 ± 0.15**
MN-CM4	2.67 ± 0.19	3.42 ± 0.17*	3.38 ± 0.39*	3.47 ± 0.26*	3.79 ± 0.45*	4.39 ± 0.69**

Values are expressed as mean ± SD for 3 observations (n=3). * $p < 0.05$, ** $p < 0.01$, *** $p < 0.001$, when equated to the respective initial after-wetting values.

Table 6: Antimicrobial activity of mangiferin chitosan alginate membrane batches

Batch No.	*Zone of inhibition (mm)*			
	A. niger	*S. aureus*	*P. aeruginosa*	*E. coli*
MN-CM1	1.45 ± 0.58	11.22 ± 0.45	17.20 ± 1.47	2.95 ± 0.32
MN-CM2	7.17 ± 0.25***	15.61 ± 0.85*	16.44 ± 1.48ns	5.18 ± 0.02***
MN-CM3	13.25 ± 0.46***	18.33 ± 2.03**	11.86 ± 0.58**	3.72 ± 0.06ns
MN-CM4	12.34 ± 1.09***	17.52 ± 0.11**	9.23 ± 1.56***	13.25 ± 1.23***

Values are expressed as mean ± SD for 3 observations (n=3). * p <0.05, ** p <0.01, *** p <0.001, and ns = not significant when equated to MN-CM1 group values.

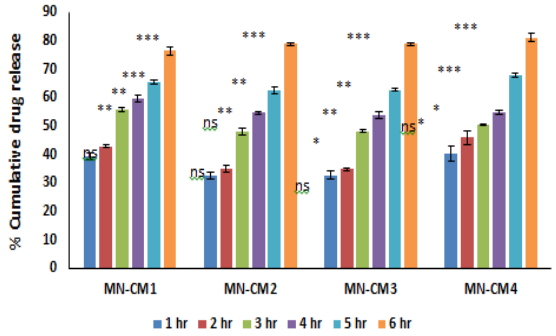

Figure 7: *In-vitro* diffusion of mangiferin chitosan alginate membrane batches

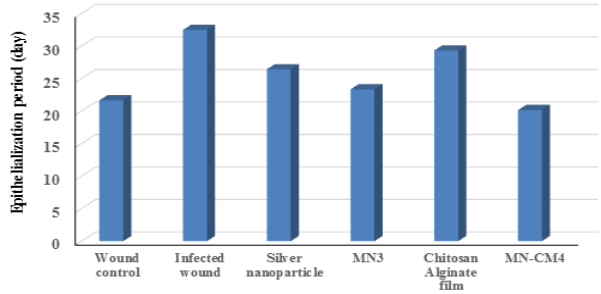

Figure 8: Effect of mangiferin Ag-NP and chitosan alginate membrane on epithelization period of infected excision in rats

Burn wound

Burn wound healing was delayed in the control group, with less than 50% wound area contraction in 21 days. Silver nanoparticle and MN3 group showed respectively 81.44 and 93.93% wound contraction by 21st day. Chitosan/alginate film and MN-CM4 showed complete healing with a 100% reduction in wound area on 21st day, confirming their superior effectiveness in wound healing (Table 8). In the burn wound group, hydroxyproline and myeloperoxidase content were respectively 29.16 µg/100 mg and 115.13 U/ml of tissue, serving as the baseline for collagen content and inflammation markers in untreated burn wounds. The hydroxyproline content has significantly (p < 0.001) increased by the silver nanoparticle, MN3, chitosan/alginate film and MN-CM4 treatment, indicating enhanced collagen synthesis. Myeloperoxidase content was reduced (p <0.001) by all the treatment groups, emphasizing the anti-inflammatory properties of Ag-NP (Figure 9).

Wound skin histopathology

In the groups treated with mangiferin Ag-NP and chitosan-alginate films, tissue regeneration began at the wound edges. In contrast, control and infected wounds exhibited diffuse bleeding and inflammatory cells. The treated groups developed a thick epidermal layer and granular tissue, while infections significantly delayed re-epithelialization. Wounds treated with mangiferin Ag-NP showed well-organized collagen strands and high-quality tissue regeneration despite a minor scab. Rats treated with mangiferin Ag-NPs and chitosan-alginate films achieved complete re-epithelialization, with normal epidermal coverage and thicker, denser collagen fibers (Figure 10).

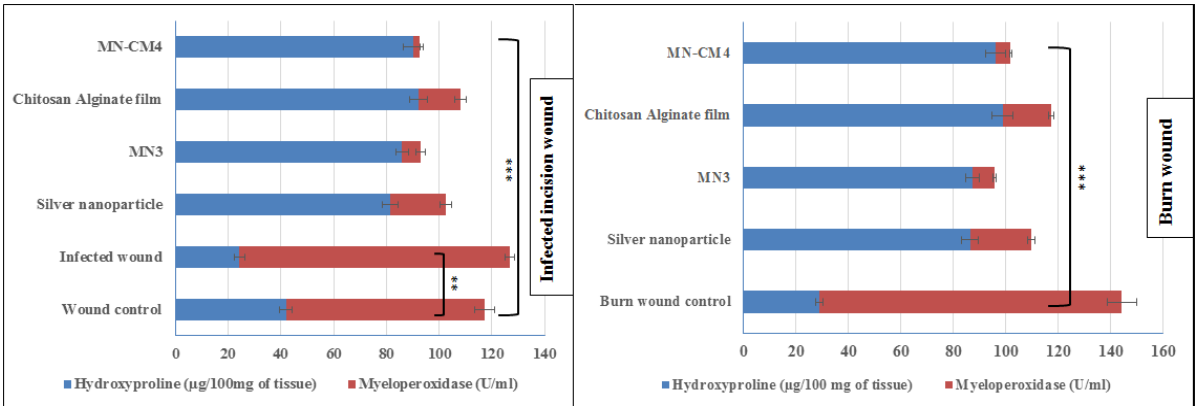

Figure 9: Effect of mangiferin Ag-NP and chitosan alginate membrane on hydroxyproline and myeloperoxidase content of infected excision and burn wound in rats

Table 7: Effect of mangiferin Ag-NP and chitosan alginate membrane on wound closure of infected excision in rats

Post-wounding days	*Wound area (mm^2) and % of wound contraction*					
	Wound control	*Infected wound*	*Silver nanoparticle*	*MN3*	*Chitosan Alginate film*	*MN-CM4*
Day 0	311.94 ± 13.90	309.45 ± 12.12	312.93 ± 15.18	321.29 ± 13.94	315.21 ± 12.01	320.25 ± 11.75
Day 1	298.56 ± 14.28^{ns}	290.66 ± 12.67^{ns}	301.87 ± 12.11^{ns}	306.25 ± 11.89^{ns}	302.48 ± 12.16^{ns}	308.16 ± 12.89^{ns}
	−4.69%	−6.07%	−3.53%	−4.68%	−4.03%	−3.77%
Day 4	286.42 ± 13.10^{ns}	524.26 ± 13.15***	442.91 ± 18.17**	289.17 ± 10.38^{ns}	412.66 ± 14.21*	205.33 ± 9.38**
	−8.18%	+69.57%	+41.53%	−10.17%	+30.92%	−35.88%
Day 7	261.62 ± 15.52^{ns}	568.33 ± 14.33***	273.73 ± 10.88^{ns}	126.2 ± 6.71***	329.33 ± 14.59^{ns}	117.1 ± 6.71***
	−16.13%	+83.65%	−12.52%	−60.72%	+4.48%	−63.43%
Day 14	215.44 ± 14.52**	399.75 ± 15.15^{ns}	122.56 ± 11.18***	59.88 ± 4.64***	265.66 ± 11.54^{ns}	48.66 ± 1.64***
	−30.93%	+29.18%	−60.83%	−81.36%	−15.72%	−84.80%
Day 21	12.89 ± 11.20***	247.66 ± 12.16^{ns}	93.56 ± 6.21***	19.53 ± 2.21***	125.21 ± 8.47***	00
	−95.86%	−18.67%	−70.10%	−93.73%	−60.27%	100%
Day 22	00	212.33 ± 10.54**	78.64 ± 4.14***	7.21 ± 1.20***	109.65 ± 6.15***	00
	100%	−31.38%	−74.86%	−97.76%	−65.21%	100%
Day 23	00	191.33 ± 5.22***	51.34 ± 2.81***	00	82.28 ± 2.95***	00
	100%	−38.17%	−83.59%	100%	−73.89%	100%

Values are expressed as Mean ± SD for 6 observations (n=3). * p <0.05, ** p <0.01, *** p <0.001, and ns = not significant when equated to day 0 values.

Table 8: Effect of mangiferin Ag-NP and chitosan alginate membrane on burn wound closure in rats

Post-wounding days	*Wound area (mm^2) and % of wound contraction*				
	Burn wound control	*Silver nanoparticle*	*MN3*	*Chitosan alginate film*	*MN-CM4*
Day 0	209.98 ± 10.12	212.63 ± 11.18	221.27 ± 13.94	215.21 ± 11.01	220.25 ± 12.75
Day 1	220.23 ± 11.67 ns	221.65 ± 12.11 ns	223.84 ± 11.89ns	212.87 ± 12.16ns	222.11 ± 11.84ns
	+4.88%	+4.24%	+1.16%	-1.09%	+0.97%
Day 4	193.19 ± 8.15 ns	122.67 ± 6.17**	199.19 ± 9.38ns	129.33 ± 8.59**	97.1 ± 7.71***
	-7.99%	-42.04%	-9.97%	-39.90%	-55.91%
Day 7	172.66 ± 7.64*	100.73 ± 5.88***	116.42 ± 9.71**	75.66 ± 5.54***	51.17 ± 3.64***
	-17.77%	-52.62%	-47.38%	-64.84%	-76.76%
Day 14	215.44 ± 14.52**	122.56 ± 11.18***	59.88 ± 4.64***	265.66 ± 11.54ns	48.66 ± 1.64***
	-30.93%	-60.83%	-81.36%	-15.72%	-84.80%
Day 21	12.89 ± 11.20***	93.56 ± 6.21***	19.53 ± 2.21***	125.21 ± 8.47***	00
	-95.86%	-70.10%	-93.73%	-60.27%	100%

Values are expressed as Mean ± SD for 6 observations (n=3). * p <0.05, ** p <0.01, *** p <0.001, and ns = not significant when equated to day 0 values.

In untreated rats, burn wounds remained unhealed with abundant inflammatory cells, necrotic tissue, and incomplete re-epithelialization. The sham chitosan-alginate film and mangiferin chitosan-alginate film-treated groups showed epidermal thickening, fewer inflammatory cells near the epidermis, and scarring with extensive collagen deposition and reduced neutrophil infiltration (Figure 10).

DISCUSSION

In this investigation, mangiferin-loaded Ag-NPs were synthesized and further embedded in chitosan alginate films. The synthesized Ag-NP underwent characterization for parameters including particle size, ZP, %EE, production yield, as well as SEM, TEM, and stability assessment. The observed particle size of the Ag-NP was below 100 nm, with satisfactory production yields across all batches. Notably, the MN3 batch exhibited the highest production yield at 74.18 ± 1.08% and demonstrated a drug entrapment efficiency of 77.42 ± 0.93%, deemed sufficiently high for incorporation into chitosan alginate films.

SEM and TEM analyses revealed small, spherical nanoparticles. Following the International Council for

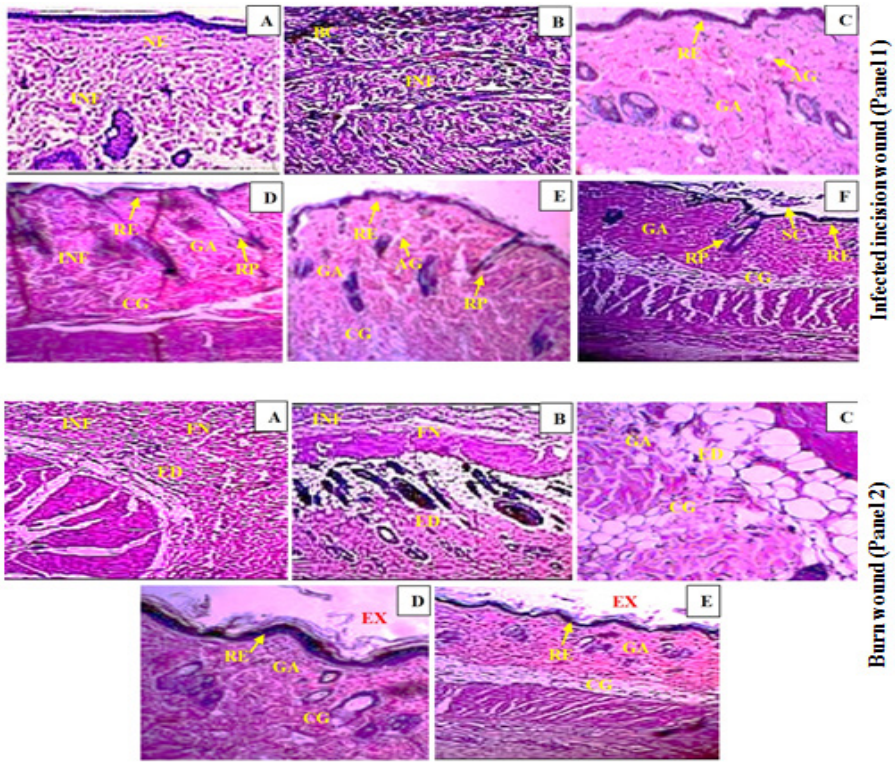

AG (angiogenesis), BC (bacterial colonies), CG (collagen), ED (edema), EX (exudate), FN (fibrinoid necrosis), GA (granulation), INF (inflammation), NE (necrosis), RE (re-epithelization), RP (rete pegs) and SC (Scab)

Figure 10: Histology of infected excision wound sections stained with hematoxylin and eosin. Epithelialization at wound control (A); Infected wound control (B); Silver nanoparticle (C); MN3 (D); Chitosan Alginate Film (E) and MN-CM4 (F) on 14th day (Panel 1).
Histology of burn wound sections stained with hematoxylin and eosin. Epithelialization at wound control (A); Silver nanoparticle (B); MN3 (C); Chitosan Alginate Film (D) and MN-CM4 (E) on 14th day (Panel 2).

Harmonisation (ICH) guidelines, the prepared nanoparticles were found to be stable, exhibiting negligible changes in evaluation parameters over a three-month period. Chitosan alginate films embedded with mangiferin-loaded Ag-NP were further assessed for film thickness, pH, average weight, %water uptake, drug content uniformity, and *in-vitro* drug release kinetics. Consistent film thicknesses were observed across all prepared films, with minimal pH variations. This uniformity in thickness indicates a correct preparation method and is a crucial technological parameter. The ability of an antibacterial film to swell is an imperative parameter for its effective biomedical use. While uniform drug content was evident in all batches, the MN-CM4 batch exhibited the highest drug content percentage at 97.33%. Notably, MN3 and MN4 batches displayed a significant increase in drug release percentage. The antibacterial efficacy of mangiferin-loaded chitosan alginate films showed substantial zones of inhibition against both gram-positive and gram-negative bacteria.

This environmentally friendly synthesized Ag-NP incorporated into chitosan alginate dressings showed superior topical effects in wound healing, owing to the synergistic action of Ag-NP and chitosan. The topical application offers advantages for example, easy application, localized effects, minimal systemic side effects, and direct visualization of the wound healing process. This approach to synthesizing films utilizing Ag-NP holds promise for expediting the healing of chronic wounds.

Chitosan exhibits broad-spectrum antibacterial properties against fungi, yeasts, and Gram-positive and Gram-negative bacteria. Its effectiveness is influenced by factors such as molecular weight, pH, ionic strength, and degree of deacetylation (DD). Because of its lower molecular weight chitosan is more soluble and more easily penetrates bacterial cell walls and ultimately shows stronger antibacterial action. Chitosan has many pathways for its antibacterial effect, i.e., bacterial cell membrane disruption initiating cell death; Chitosan can prevent bacterial growth and biofilm development by chelating metal ions obstructing the capacity of bacteria to colonies surfaces and cause infection. Interferes with microbial gene expression and also produces reactive oxygen species (ROS), initiating oxidative stress and eventually killing the cells.[51]

The antimicrobial activity of optimized chitosan alginate film (MN-CM4) was determined against the most frequently found bacteria in infected skin wounds. Consequently, the silver nanoparticle-loaded film was evaluated as a wound dressing due to its strong antibacterial and anti-inflammatory properties.[52,53]

In the infected excision wound model, MN3-treated rats showed a significant reduction in wound area compared to control groups, with faster contraction from day 7 to day 21. The MN-CM4 group achieved 100% wound contraction by day 21, starting from day 7. The superior contraction rate in the MN-CM4 group is likely due to its combined effects on cell proliferation, collagen synthesis, moisture retention, infection control, and anti-inflammatory properties. Additionally, the epithelialization period was notably reduced from 23 days (MN3) to 19 days for the MN-CM4 group. The shorter epithelialization time and accelerated wound contraction may result from the enhanced antimicrobial activity of Ag-NP, the bioactivity of chitosan and alginate, improved collagen synthesis, stimulated cell proliferation, and the antioxidant and antibacterial effects of mangiferin. These materials work synergistically to create an optimal environment for wound healing, supporting faster tissue regeneration and reducing the risk of infection.[54]

The high myeloperoxidase activity in the infected wound control group demonstrates the typical inflammatory response to infection. However, the marked decrease in myeloperoxidase levels with MN3 and MN-CM4 suggests their potential in managing infection-induced inflammation. The synergistic effects of mangiferin with either Ag-NP or chitosan alginate result in the lowest myeloperoxidase activities observed. This underscores the potential of these combinations in providing enhanced anti-inflammatory and antimicrobial effects, making them promising candidates for advanced wound care therapies. Collagen synthesis, evaluated by hydroxyproline measurement, showed higher values for the chitosan alginate film and MN-CM4 treated groups. These results indicate stimulation of collagen production by chitosan alginate and mangiferin. The presence of thicker as well as supplementary systematized collagen fibers suggests that the biomaterial plays a crucial role in the wound bed throughout all stages of healing.[55]

The burn wound healing effect in the MN-CM4 group is likely due to accelerated re-epithelialization, neovascularization, free radical scavenging, inflammation reduction, and infection control, thanks to the antioxidant, anti-inflammatory, and antimicrobial properties of mangiferin and chitosan-alginate. This combined treatment not only enhances cellular protection and tissue repair but also creates a cleaner wound environment, facilitating comprehensive and effective wound healing. Decreased hydroxyproline content, along with increased myeloperoxidase, highlights the detrimental impact of infection on collagen synthesis and overall wound healing. The MN-CM4 group showed a high hydroxyproline content, demonstrating that the combination of mangiferin with chitosan alginate significantly enhances collagen synthesis, matching the efficacy of the chitosan alginate film alone. The combination of mangiferin with chitosan alginate (MN-CM4) appears to be highly effective in reducing inflammation.[52-55]

Mangiferin's anti-inflammatory effects involve inhibiting IRAK1, NF-κB, and MAPK phosphorylation, upregulating COX-2, inducing nitric oxide synthase, and suppressing TNF-α, IL-1β, and IL-6. It also downregulates mRNA expression of pro-inflammatory mediators like iNOS and IL-6 and inhibits NF-κB p65 and ICAM-1 phosphorylation. Mangiferin mitigates oxidative stress by stabilizing free radicals and reducing COX-2, PGE2, LTB4, and cytokines such as TNF-α, IL-4, and IL-5.[51-55]

The inflammatory phase of wound healing can be significantly affected by bacterial infections, oxidative stress, and poor hygiene. Once the epithelium is compromised, various microorganisms, including bacteria, fungi, and antigens, can lead to critical infections. Wound infections are commonly associated with four bacterial strains: *S. aureus, Streptococcus* species, *E. coli*, and *P. aeruginosa*. These bacteria produce endotoxins that increase the levels of pro-inflammatory cytokines for example, IL-1 and TNF-α, potentially initiating the wound to enter a chronic state and hindering healing. Some flavones can reduce quorum sensing (QS) in *P. aeruginosa* (strain PAO1), disrupting biofilm formation. Additionally, mangiferin has been reported to have iron-chelating activity, which is crucial for bacterial growth, as iron is essential for enzymes involved in DNA synthesis.[56]

Mangiferin, a bioactive phytoconstituent, was used for wound healing in combination with silver nanoparticles and chitosan alginate film to enhance wound healing and anti-inflammatory, antioxidant, and antimicrobial properties. The silver nanoparticle of mangiferin has broad-spectrum antimicrobial activity. The nanoparticles provide a sustained release of silver ions, which helps to prevent and treat infections at the wound site. Chitosan and alginate are natural polymers that are biocompatible and biodegradable, making them suitable for wound dressings. They form a gel-like film that adheres well to the wound place, providing a humid atmosphere. Cs/Alg film of mangiferin silver nanoparticle gives a synergistic effect of wound healing. The study's findings indicate that the chitosan-alginate film containing mangiferin Ag-NPs significantly enhances wound healing in both infected excision and burn wound models.[56]

CONCLUSION

This study successfully synthesized and characterized mangiferin-loaded Ag-NP (Ag-NPs), which were subsequently embedded into chitosan-alginate (Cs/Alg) films for advanced wound care applications. The mangiferin was isolated with a 1.3% yield, forming pale-yellow needle-shaped crystals with a melting point of 270 to 272ºC. TLC, UV-visible, FTIR, and HPLC analyses confirmed the purity and structure of the mangiferin. The synthesized Ag-NPs, particularly the MN3 batch, displayed small particle size (36.60 ± 0.91 nm), high stability (ZP of -29.10 mV), and significant %EE (77.42%) and yield (74.18%). SEM and TEM confirmed the spherical and smooth morphology of these nanoparticles. Stability tests showed no significant changes in particle size, ZP, and %EE over three months. The Cs/Alg films exhibited appropriate thickness, weight, water uptake, and pH changes, with MN-CM4 showing the highest performance. *In-vitro* drug release studies indicated a significant increase in release, especially in MN-CM4, which also demonstrated the highest

antibacterial activity. *In-vivo* studies on excision and burn wound models revealed that MN-CM4 facilitated complete wound closure by day 21, improved hydroxyproline levels, reduced myeloperoxidase content, and promoted better tissue regeneration. These conclusions highlight the potential of mangiferin-loaded Ag-NPs in enhancing wound healing through their anti-inflammatory and antibacterial properties.

REFERENCES

1. Allaw M, Pleguezuelos-Villa M, Manca ML, Caddeo C, Aroffu M, Nacher A, Diez-Sales O, Saurí AR, Ferrer EE, Fadda AM, Manconi M. Innovative strategies to treat skin wounds with mangiferin: Fabrication of transfersomes modified with glycols and mucin. Nanomedicine. 2020 Jul 1;15(17):1671-85. DOI: https://doi.org/10.2217/nnm-2020-0116
2. Al-Samydai A, Qaraleh MA, Alshaer W, Al-Halaseh LK, Issa R, Alshaikh F, Abu-Rumman A, Al-Ali H, Al-Dujaili EA. Preparation, characterization, wound healing, and cytotoxicity assay of PEGylated nanophytosomes loaded with 6-gingerol. Nutrients. 2022 Dec 5;l4(23):5170. DOI: https://doi.org/10.3390/nu14235170
3. Ameen F, Srinivasan P, Selvankumar T, Kamala-Kannan S, Al Nadhari S, Almansob A, Dawoud T, Govarthanan M. Phytosynthesis of Ag-NP utilizing *Mangifera indica* flower extract as bioreductant and their broad-spectrum antibacterial activity. Bioorganic Chemistry. 2019 Jul 1;88:102970. DOI: https://doi.org/10.1016/j.bioorg.2019.102970
4. Bayda S, Adeel M, Tuccinardi T, Cordani M, Rizzolio F. The history of nanoscience and nanotechnology: from chemical–physical applications to nanomedicine. Molecules. 2019 Dec 27;25(1):112. DOI: https://doi.org/10.3390/molecules25010112
5. Bilgen F, Ural A, Kurutas EB, Bekerecioglu M. The effect of oxidative stress and Raftlin levels on wound healing. International wound journal. 2019 Oct;16(5):1178-84. DOI: https://doi.org/10.1111/iwj.13177
6. Caetano GF, Frade MA, Andrade TA, Leite MN, Bueno CZ, Moraes ÂM, Ribeiro-Paes JT. Chitosan-alginate membranes accelerate wound healing. Journal of Biomedical Materials Research Part B: Applied Biomaterials. 2015 Jul;103(5):1013-22. DOI: https://doi.org/10.1002/jbm.b.33277
7. Chalitangkoon J, Wongkittisin M, Monvisade P. Silver loaded hydroxyethylacryl chitosan/sodium alginate hydrogel films for controlled drug release wound dressings. International journal of biological macromolecules. 2020 Sep 15;159:194-203. DOI: https://doi.org/10.1016/j.ijbiomac.2020.05.061
8. Dananjaya SH, Kulatunga DC, Godahewa GI, Nikapitiya C, Oh C, Edussuriya M, Lee J, De Zoysa M. Preparation, characterization, and antimicrobial properties of chitosan–silver nanocomposites films against fish pathogenic bacteria and fungi. Indian journal of microbiology. 2017 Dec;57:427-37. DOI: https://doi.org/10.1007/s12088-017-0670-4
9. Dar A, Faizi S, Naqvi S, Roome T, Zikr-ur-Rehman S, Ali M, Firdous S, Moin ST. Analgesic and antioxidant activity of mangiferin and its derivatives: the structure activity relationship. Biological and Pharmaceutical Bulletin. 2005;28(4):596-600. DOI: https://doi.org/10.1248/bpb.28.596
10. Das J, Ghosh J, Roy A, Sil PC. Mangiferin exerts hepatoprotective activity against D-galactosamine induced acute toxicity and oxidative/nitrosative stress via Nrf2–NFκB pathways. Toxicology and applied pharmacology. 2012 Apr 1;260(1):35-47. DOI: https://doi.org/10.1016/j.taap.2012.01.015
11. Daud NH, Aung CS, Hewavitharana AK, Wilkinson AS, Pierson JT, Roberts-Thomson SJ, Shaw PN, Monteith GR, Gidley MJ, Parat MO. Mango extracts and the mango component mangiferin promote endothelial cell migration. Journal of agricultural and food chemistry. 2010 Apr 28;58(8):5181-6. DOI: https://doi.org/10.1021/jf100249s
12. Demilew W, Adinew GM, Asrade S. Evaluation of the wound healing activity of the crude extract of leaves of Acanthus polystachyus Delile (Acanthaceae). Evidence-Based Complementary and Alternative Medicine. 2018;2018(1):2047896. DOI: https://doi.org/10.1155/2018/2047896
13. Dou W, Zhang J, Ren G, Ding L, Sun A, Deng C, Wu X, Wei X, Mani S, Wang Z. Mangiferin attenuates the symptoms of dextran sulfate sodium-induced colitis in mice via NF-κB and MAPK signaling inactivation. International immunopharmacology. 2014 Nov 1;23(1):170-8. DOI: https://doi.org/10.1016/j.intimp.2014.08.025
14. Du S, Liu H, Lei T, Xie X, Wang H, He X, Tong R, Wang Y. Mangiferin: An effective therapeutic agent against several disorders. Molecular medicine reports. 2018 Dec 1;18(6):4775-86. DOI: https://www.spandidos-publications.com/mmr/18/6/4775
15. Eldin MM, Hashem AE, Tamer TM, Omer AM, Yossuf ME, Sabet MM. Development of cross linked chitosan/alginate polyelectrolyte proton exchanger membranes for fuel cell applications. International Journal of Electrochemical Science. 2017 Feb 1;12(5):3840-58. DOI: https://doi.org/10.20964/2017.05.45
16. Engels C, KNOdler MA, Zhao YY, Carle R, Gänzle MG, Schieber A. Antimicrobial activity of gallotannins isolated from mango (*Mangifera indica* L.) kernels. Journal of agricultural and food chemistry. 2009 Sep 9;57(17):7712-8. DOI: https://doi.org/10.1021/jf901621m
17. Espinosa-Espinosa L, Garduño-Siciliano L, Rodriguez-Canales M, Hernandez-Portilla LB, Canales-Martinez MM, Rodriguez-Monroy MA. The wound-healing effect of mango peel extract on incision wounds in a murine model. Molecules. 2022 Jan 1;27(1):259. DOI: https://doi.org/10.3390/molecules27010259
18. Ferranti-Ramos A, Garza-Garza G, Bátiz-Armenta J, Martínez-Delgado G, la Garza-Álvarez D, Martínez-Menchaca HR, Rivera-Silva G. Metaloproteinasas de la matriz extracelular y su participación en el proceso de cicatrización. Medicas UIS. 2017 Aug;30(2):55-62. DOI: http://dx.doi.org/10.18273/revmed.v30n2-2017006
19. Gantwerker EA, Hom DB. Skin: histology and physiology of wound healing. Clinics in plastic surgery. 2012 Jan 1;39(1):85-97. DOI: https://doi.org/10.1016/j.cps.2011.09.005
20. Garcia D, Leiro J, Delgado R, Sanmartin ML, Ubeira FM. *Mangifera indica* L. extract (Vimang) and mangiferin modulate mouse humoral immune responses. Phytotherapy Research: An International Journal Devoted to Pharmacological and Toxicological Evaluation of Natural Product Derivatives. 2003 Dec;17(10):1182-7. DOI: https://doi.org/10.1002/ptr.1338
21. Garrido G, González D, Lemus Y, Garcıa D, Lodeiro L, Quintero G, Delporte C, Núñez-Sellés AJ, Delgado R. *In-vivo* and *in-vitro* anti-inflammatory activity of *Mangifera indica* L. extract (VIMANG®). Pharmacological research. 2004 Aug 1;50(2):143-9. DOI: https://doi.org/10.1016/j.phrs.2003.12.003
22. Han J, Yi J, Liang F, Jiang B, Xiao Y, Gao S, Yang N, Hu H, Xie WF, Chen W. X-3, a mangiferin derivative, stimulates AMP-

activated protein kinase and reduces hyperglycemia and obesity in db/db mice. Molecular and Cellular Endocrinology. 2015 Apr 15;405:63-73. DOI: https://doi.org/10.1016/j.mce.2015.02.008
23. European Medicines Agency. ICH Topic Q1A (R2) Stability Testing of New Drug Substances and Products. August 2003; CPMP/ICH/2736/99.
24. Janigová N, Elbl J, Pavloková S, Gajdziok J. Effects of Various Drying Times on the Properties of 3D Printed Orodispersible Films. Pharmaceutics. 2022 Jan 21;14(2):250. DOI: https://doi.org/10.3390/pharmaceutics14020250
25. Jeong JJ, Jang SE, Hyam SR, Han MJ, Kim DH. Mangiferin ameliorates colitis by inhibiting IRAK1 phosphorylation in NF-κB and MAPK pathways. European Journal of Pharmacology. 2014 Oct 5;740:652-61. DOI: https://doi.org/10.1016/j.ejphar.2014.06.013
26. Johnson TR, Gómez BI, McIntyre MK, Dubick MA, Christy RJ, Nicholson SE, Burmeister DM. The cutaneous microbiome and wounds: new molecular targets to promote wound healing. International journal of molecular sciences. 2018 Sep 11;19(9):2699. DOI: https://doi.org/10.3390/ijms19092699
27. Jyotshna, Khare P, Shanker K. Mangiferin: A review of sources and interventions for biological activities. BioFactors. 2016 Sep 10;42(5):504-14. DOI: https://iubmb.onlinelibrary.wiley.com/doi/abs/10.1002/biof.1308
28. Keshari AK, Srivastava R, Singh P, Yadav VB, Nath G. Antioxidant and antibacterial activity of Ag-NP synthesized by Cestrum nocturnum. Journal of Ayurveda and integrative medicine. 2020 Jan 1;11(1):37-44. DOI: https://doi.org/10.1016/j.jaim.2017.11.003
29. Khubiev OM, Egorov AR, Kirichuk AA, Khrustalev VN, Tskhovrebov AG, Kritchenkov AS. Chitosan-based antibacterial films for biomedical and food applications. International Journal of Molecular Sciences. 2023 Jun 27;24(13):10738. DOI: https://doi.org/10.3390/ijms241310738
30. Khurana RK, Rao S, Beg S, Katare OP, Singh B. Systematic development and validation of a thin-layer densitometric bioanalytical method for estimation of mangiferin employing analytical quality by design (AQbD) approach. Journal of Chromatographic Science. 2016 May 1;54(5):829-41. DOI: https://academic.oup.com/chromsci/article/54/5/829/1745060
31. Lwin OM, Giribabu N, Kilari EK, Salleh N. Topical administration of mangiferin promotes healing of the wound of streptozotocin-nicotinamide-induced type-2 diabetic male rats. Journal of Dermatological Treatment. 2021 Nov 17;32(8):1039-48. DOI: https://doi.org/10.1080/09546634.2020.1721419
32. Mahendran S, Badami S, Ravi S, Thippeswamy BS, Veerapur VP. Synthesis and evaluation of analgesic and anti-inflammatory activities of most active free radical scavenging derivatives of mangiferin. British Journal of Applied Science & Technology. 2014 Jan 10;4(35):4959-73. DOI: https://doi.org/10.9734/BJAST/2014/12745
33. Furniss BS, Hannaford AJ, Smith PWG, Tatchell AR. Vogel's, Textbook of Practical Organic Chemistry, 5th edition, Longman Scientific and Technical, England. 1989: 236-240. DOI: https://faculty.ksu.edu.sa/sites/default/files/vogel_-_practical_organic_chemistry_5th_edition.pdf
34. Biswas T, Sen A, Roy R, Maji S, Maji HS. Isolation of mangiferin from flowering buds of *Mangifera indica* L and its evaluation of *in-vitro* antibacterial activity. J Pharm Anal. 2015;4(3):49-56. DOI: http://dx.doi.org/10.9755/ejfa.v26i7.18188
35. Meng X, Tian F, Yang J, He CN, Xing N, Li F. Chitosan and alginate polyelectrolyte complex membranes and their properties for wound dressing application. Journal of Materials Science: Materials in Medicine. 2010 May;21:1751-9. DOI: https://doi.org/10.1007/s10856-010-3996-6
36. Espinosa-Espinosa L, Garduño-Siciliano L, Rodriguez-Canales M, Hernandez-Portilla LB, Canales-Martinez MM, Rodriguez-Monroy MA. The wound-healing effect of mango peel extract on incision wounds in a murine model. Molecules. 2022 Jan 1;27(1):259. DOI: https://doi.org/10.3390/molecules27010259
37. Muruganandan S, Lal J, Gupta PK. Immunotherapeutic effects of mangiferin mediated by the inhibition of oxidative stress to activated lymphocytes, neutrophils and macrophages. Toxicology. 2005 Nov 5;215(1-2):57-68. DOI: https://doi.org/10.1016/j.tox.2005.06.008
38. Nnamdi O. Development and characterization of mucoadhesive patches for buccal delivery of pregabalin. Universal Journal of Pharmaceutical Research. 2017 May 1. 2017;2(3):6-9. DOI: https://doi.org/10.22270/ujpr.v2i3.R2
39. Othman SN, Seka M. In-vitro antioxidant and cytotoxic activities of Ag-NP of mangiferin isolated from *Mangifera indica*. Journal of Global Pharma Technology. 2019;11(6):10-5. DOI: http://www.jgpt.co.in/
40. Pansara C, Mishra R, Mehta T, Parikh A, Garg S. Formulation of chitosan stabilized silver nanoparticle-containing wound healing film: *in-vitro* and *in-vivo* characterization. Journal of pharmaceutical sciences. 2020 Jul 1;109(7):2196-205. DOI: https://doi.org/10.1016/j.xphs.2020.03.028
41. Paul W, Sharma CP. Chitosan and alginate wound dressings: a short review. Trends Biomater Artif Organs. 2004 Jul 1;18(1):18-23. DOI: https://tarjomefa.com/wp-content/uploads/2016/09/5300-English.pdf
42. Prajapati B, Raichandani Y, Patel R, Sawant K. Chitosan alginate film for topical drug delivery of antimicrobial agents. Curr Pharma Res J. 2007;1(03):66-74. DOI: https://www.researchgate.net/publication/291116073_Chitosan_Alginate_Film_For_Topical_Drug_Delivery_Of_Antimicrobial_Agents
43. Rajendran P, Ekambaram G, Magesh V, Sakthisekaran D. Chemopreventive efficacy of mangiferin against benzo (a) pyrene induced lung carcinogenesis in experimental animals. Environmental Toxicology and Pharmacology. 2008 Nov 1;26(3):278-82. DOI: https://doi.org/10.1016/j.etap.2008.05.005
44. Rasyid R, Ruslan R, Mawaddah S, Rivai H. Quantitative determination of mangiferin in methanol extract of bacang mango (Mangifera foetida L.) leaves by thin-layer chromatography densitometry. World Journal of Pharmacy and Pharmaceutical Sciences.2020; 9(7):1551-1560. DOI: http://www.wjpps.com/
45. Samadarsi R, Dutta D. Design and characterization of mangiferin nanoparticles for oral delivery. Journal of Food Engineering. 2019 Apr 1;247:80-94. DOI: https://doi.org/10.1016/j.jfoodeng.2018.11.020
46. Sharma S, Sanpui P, Chattopadhyay A, Ghosh SS. Fabrication of antibacterial silver nanoparticle—sodium alginate–chitosan composite films. Rsc Advances. 2012;2(13):5837-43. DOI: https://doi.org/10.1039/C2RA00006G
47. Sushanth KA, Lakshmi KC, Reddy DS. Evaluation of wound healing activity with a new formulation of dry *Mangifera indica* and honey utilizing swiss albino mice. Asian Journal of Pharmaceutical and Clinical Research. 2016 Jul 1:139-42. DOI: file:///C:/Users/admin/Downloads/admin,+Journal+manager,+A

JPCR_11810_RA.pdf
48. Tenorová K, Masteiková R, Pavloková S, Kostelanská K, Bernatonienė J, Vetchý D. Formulation and evaluation of novel film wound dressing based on collagen/microfibrillated carboxymethylcellulose blend. Pharmaceutics. 2022 Apr 3;14(4):782. DOI: https://doi.org/10.3390/pharmaceutics14040782
49. Vandeputte OM, Kiendrebeogo M, Rasamiravaka T, Stevigny C, Duez P, Rajaonson S, Diallo B, Mol A, Baucher M, El Jaziri M. The flavanone naringenin reduces the production of quorum sensing-controlled virulence factors in Pseudomonas aeruginosa PAO1. Microbiology. 2011 Jul;157(7):2120-32. DOI: https://doi.org/10.1099/mic.0.049338-0
50. Vyas A, Syeda K, Ahmad A, Padhye S, H Sarkar F. Perspectives on medicinal properties of mangiferin. Mini Reviews in Medicinal Chemistry. 2012 May 1;12(5):412-25. DOI: https://doi.org/10.2174/138955712800493870
51. Zhang X, Su B, Li J, Li Y, Lu D, Zhu K, Pei H, Zhao M. Analysis by RP-HPLC of mangiferin component correlation between medicinal loranthus and their mango host trees. Journal of Chromatographic Science. 2014 Jan 1;52(1):1-4. DOI: https://doi.org/10.1093/chromsci/bms196
52. Zhu XM, Song JX, Huang ZZ, Wu YM, Yu MJ. Antiviral activity of mangiferin against herpes simplex virus type 2 *in-vitro*. Zhongguo yao li xue bao= Acta Pharmacologica Sinica. 1993 Sep 1;14(5):452-4. DOI: https://europepmc.org/article/med/8010041
53. Kadhim O, Al-demirchi JY, Al-Hussainawy MK, Al-Hamdani MM, Kadhim AJ. Efficiency of Phenazine Compound Produced by Rhizospheric Pseudomonas fluorescens against Few Pathogenic Bacteria Isolated from Ear Infections. International Journal of Drug Delivery Technology. 2023;13(4):1167-1171. DOI: 10.25258/ijddt.13.4.07
54. Ismail WF, Al-Mudhafar MMJ, Fadhil AA, Synthesis, Characterization of New Isatin-Ibuprofen Derivatives with Expected Biological Activity. International Journal of Drug Delivery Technology. 2022;12(4):1560-1565. DOI: 10.25258/ijddt.12.4.13
55. Mohammed RH, Al-Niaame AE. Evaluation of the Biological Efficacy and Physicochemical Evaluation of Toothpaste Prepared from Few Types of Plant Extracts against Some Pathogenic Bacteria Isolated from the Mouth. International Journal of Drug Delivery Technology. 2022;12(4):1626-1631. DOI: 10.25258/ijddt.12.4.25
56. Mathew S, Sankarganesh P, Joseph B. Ecotoxicological Effects of Lead Exposed Cyprinus carpio and HSP70-Induced Antioxidants against ROS. International Journal of Drug Delivery Technology. 2023;13(4):1178-1182. DOI: 10.25258/ijddt.13.4.09